Improved-Accuracy Source Reconstructionon Arbitrary 3-D Surfaces

(Article begins on next page)

29 September 2022

# Near- and Very Near-Field Accuracy in 3-D Source Reconstruction

Javier Leonardo Araque Quijano and Giuseppe Vecchi, *Fellow, IEEE*

*Abstract*—We present a quantitative assessment of the accuracy in reconstructing the near fields from assigned field data with various source reconstruction formulations. Accurate and robust computation of near fields is of great interest in diagnostic applications from real measurements, which are unavoidably affected by noise and/or measurement uncertainties. Tests are performed with finite signal-to-noise ratio (SNR) synthetic data and with measured data; they indicate that only the recently introduced dual-equation formulation provides a reliable reconstruction of fields in the close vicinity of the equipment under test.

*Index Terms*—Antenna diagnostics, inverse problems, inverse source, source reconstruction.

## I. INTRODUCTION AND MOTIVATIONS

IN source reconstruction, one sets a surface around the antenna under test (AUT) and looks for equivalent sources on it that radiate a field distribution specified at a given (further) surface; the field is usually specified by measurements, and the associated surface is thus called "measurement surface," while the surface where sources are sought is called "reconstruction surface." Source reconstruction is a valuable tool in antenna diagnostics and near-field to far-field (NF–FF) transformation that provides a unified treatment with virtually no geometrical constrains of both measurement and reconstruction surfaces. It is therefore more flexible than techniques based on the simpler wave expansion, although the geometric capabilities of the latter can be extended in some cases through wave re-expansion (e.g., as in [1]). On the negative side, computational complexity is considerably increased; a more subtle difficulty is associated to its generality and less direct link between measured and reconstructed *fields*. The technique is more difficult to characterize from the theoretical point of view, complicating its correct use.

Among the several works found in literature on the subject, we attempt here a nonoverlapping account of the various mathematical formulations for arbitrary 3-D surfaces, leaving out the very many specific application instances that can be found in the referenced works. In what follows, we will not consider works dealing with (2-D) reconstruction on a (infinite) plane. The most widespread approach is the one in [2] and [3]; in these, equivalent electric and magnetic sources are reconstructed on a given surface with the only constraint that they radiate the measured fields, thus resulting in a single-equation formulation (SEqF). Efficient large-scale implementation of this approach is presented in [4]. In an alternative approach, the condition above is augmented with the enforcement of Love's equivalence form, thus resulting in a dual-equation formulation (DEqF); this was done in [5] for the scalar case using a dual-surface approach, while [6] presented the general vector 3-D formulation with on-surface boundary integral identities. A special version of the latter was subsequently presented in [7] for the case of axisymmetric geometries. Finally, [8] unified the above formulations into a general theoretical framework and introduced a third formulation, in which the Equivalence Theorem is used to deal with one equivalent source only (still on a 3-D surface); as reported there, this equivalent source is not a Love's source.

It was pointed out in [8] that the more conventional formulation [2] does not yield Love's currents, and therefore the obtained equivalent currents do not represent the fields on the reconstruction surfaces. Once this misunderstanding is removed, and it is recognized that these currents are one of the (infinitely many) possible choices of the Equivalence Theorem [8], one can conjecture that all three approaches above will yield the same fields everywhere *outside* the reconstruction surface, via proper radiation from the found sources—as per the Equivalence Theorem. Whether this happens in practice is far from trivial: The equivalent sources result from the solution of a discretized ill-posed problem, and the input field derives from measurements with finite precision.

Motivated by the above, we present here a quantitative evaluation of the accuracy in reconstructing the fields near the reconstruction surface and farther away. We compare various formulations of the source reconstruction technique with a main focus on near-field to near-field (NF–NF) transformation applications, which are of great interest in the diagnostics of antennas and other devices. To the best of our knowledge, such an assessment is missing in literature, and yet it is necessary information for a practical use of source reconstruction. It should be noted that NF–NF applications pose a more challenging task than NF–FF. In fact, when one is interested in a representation of fields valid outside the measurement surface (as in NF–FF), a good fitting of the measured data suffices, provided it is sampled according to the EM field degrees of freedom (FDoF). The situation is quite different when one wants to look inside, in particular in the close vicinity of reconstructed currents, as required, e.g., in the diagnostics of antenna arrays to determine amplitude, phase and/or polarization anomalies, and in general sources of spurious radiation.

## II. BACKGROUND

The formulation of source reconstruction problem has been dealt with in previous literature, and we limit ourselves here to reporting the expressions relevant to our present endeavor; the interested reader can further refer to [6] and [8]. The aim is to compute equivalent currents on a closed reconstruction surface $\Sigma_R$ from knowledge of complex vector field samples scattered on an open or closed measurement surface $\Sigma_M$. All formulations involve the electric field integral equation (EFIE) ($\mathcal{L}$) and/or magnetic field integral equation (MFIE) ($\mathcal{K}$) operators

$$\mathcal{L}(\mathbf{J}; \mathbf{r}) = jk_0 \int_{\Sigma_R} \left[ \mathbf{J}(\mathbf{r}') + \frac{1}{k_0^2} \nabla \nabla'_s \cdot \mathbf{J}(\mathbf{r}') \right] g(\mathbf{r}, \mathbf{r}') ds'$$

$$\mathcal{K}(\mathbf{M}; \mathbf{r}) = \int_{\Sigma_R} \mathbf{M}(\mathbf{r}') \times \nabla g(\mathbf{r}, \mathbf{r}') ds'$$

$$g(\mathbf{r}, \mathbf{r}') = \frac{e^{-jk_0 |\mathbf{r}-\mathbf{r}'|}}{4\pi |\mathbf{r}-\mathbf{r}'|} \quad (1)$$

with $\eta_0 = \sqrt{\mu_0/\epsilon_0}$, $k_0 = \omega\sqrt{\mu_0\epsilon_0}$.

Conventional SEqF only enforces that the equivalent currents $\mathbf{J}$ and $\mathbf{M}$ radiate the fields measured on $\Sigma_M$ to compute the former

$$\hat{\mathbf{n}} \times \mathbf{E}(\mathbf{r}) = \hat{\mathbf{n}} \times [-\eta_0 \mathcal{L}(\mathbf{J}; \mathbf{r}) + \mathcal{K}(\mathbf{M}; \mathbf{r})], \quad \mathbf{r} \in \Sigma_M. \quad (2)$$

As discussed in [8], single-current formulations are obtained enforcing continuity of one of the fields across $\Sigma_R$, which results in keeping only $\mathbf{J}$ or only $\mathbf{M}$ in (2); these will be termed J-current single-equation formulation (J-SEqF) and M-current single-equation formulation (M-SEqF).

In Love's equivalence, the unknown currents obey $\mathbf{M}^{\text{Love}} = -\hat{\mathbf{n}} \times \mathbf{E}$ and $\mathbf{J}^{\text{Love}} = \hat{\mathbf{n}} \times \mathbf{H}$ on the outer side of $\Sigma_R$, equivalent to state that they radiate identically zero field inside $\Sigma_R$; this additional requirement results in [6]

$$\hat{\mathbf{n}} \times [-\eta_0 \mathcal{L}(\mathbf{J}^{\text{Love}}; \mathbf{r}) + \mathcal{K}(\mathbf{M}^{\text{Love}}; \mathbf{r})] = -\frac{1}{2}\mathbf{M}^{\text{Love}}(\mathbf{r}), \quad \mathbf{r} \in \Sigma_R. \quad (3)$$

Equation (3) is just one of the possible forms to impose Love's equivalence [6]. The implementation used for the tests in subsequent sections [and in particular the approximate evaluation of (3)] is as in [6] and thus is not repeated here.

## III. ACCURACY TESTS

For the tests, we employ a structure for which: 1) measured data was available; and 2) full-wave (method of moments, MoM) simulation is possible so that synthetic data can be generated for a comprehensive quantitative near-field assessment. The test structure is a monocone antenna placed above a circular ground plane that lies on the $xy$ plane, as sketched in Fig. 1.

For a meaningful comparison, throughout our tests we keep fixed the reconstruction surface $\Sigma_R$, its discretization, and the sampling points on the measurement surface $\Sigma_M$. Unknown currents are computed on an oblate ellipsoid, as seen in Fig. 1. The ellipsoidal $\Sigma_R$ is discretized by triangular facets with average cell size $h_R = 0.25\lambda$. The currents are approximated by 1251 Rao–Wilton–Glisson (RWG) basis functions. Therefore,
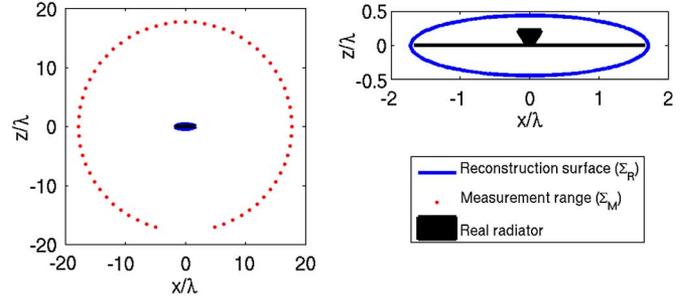


Fig. 1. Geometry for the numerical tests performed.

the single-current formulations involve 1251 current unknowns (for $\mathbf{J}$ or $\mathbf{M}$), and the two-current formulations (both single- and dual-equation) 2502 unknowns.

The measurement range is a (centered) sphere of radius $R_M = 17.7\lambda$ and presents a truncation as a result of the supporting mast: No measurements are present for $\theta \geq 164°$. The sampling is uniform in $\theta$ and $\phi$, with an angular step of $5.3°$ and a total of 4352 measurements (for the two polarizations). The overall setup is shown in Fig. 1. In the tests with synthetic data, the field is specified exactly as in the case of the measurements.

Since only the DEqF yields Love's currents, and thus fields, on the reconstruction surface, for a fair comparison we have always evaluated the fields at a finite distance from $\Sigma_R$. For the same reason, and as a mean to test robustness within an automatic tool, in all cases the resulting linear system is solved via the conjugate gradient (CG) iterative solver, which executes till residual stagnation occurs. Given the reduced dimensions of the resulting linear system, a direct solver could be used. However, we chose to employ an iterative solver in order to provide a common ground with large-scale problems—which exclude the use of direct solvers—and to take advantage of the inherent regularizing properties of the CG and similar solvers [9] (it is especially beneficial for SEqFs that have a significantly worse conditioning).

Near fields are evaluated on semi-ellipses concentric with $\Sigma_R$ and semiaxes $[s_x^{\text{nf}}, s_y^{\text{nf}}, s_z^{\text{nf}}] = [s_x, s_y, s_z] + \Delta s$ with $\Delta s$ taking on 10 values in the interval $0.1\lambda - 2.0\lambda$ as shown in Fig. 2. The indicator employed is the relative difference between reference (i.e., full-wave) near fields and those radiated by the reconstructed currents

$$\varepsilon_{\text{NF}}(\Delta s) = 10 \log_{10} \frac{\sum_n \left| E_{\text{rec}}\left(\mathbf{r}_n^{\Delta s}\right) - E_{\text{ref}}\left(\mathbf{r}_n^{\Delta s}\right) \right|^2}{\sum_n \left| E_{\text{ref}}\left(\mathbf{r}_n^{\Delta s}\right) \right|^2} \quad (4)$$

where $\mathbf{r}_n^{\Delta s}$ are sample points into the semi-ellipses as depicted in Fig. 2 for each possible value of $\Delta s$.

Finally, we report also the final value of the residual achieved by the solver, which deals with the normal equation resulting from the rectangular system (see captions of Figs. 3 and 5).

### A. Sensitivity Tests With Synthetic Data

For the first group of tests, we perform source reconstruction from data generated synthetically. A simplified computer-aided design (CAD) model of the real radiator is simulated via MoM so that fields at any location can be computed, in particular the synthetic measurements on $\Sigma_M$ and reference near field at the
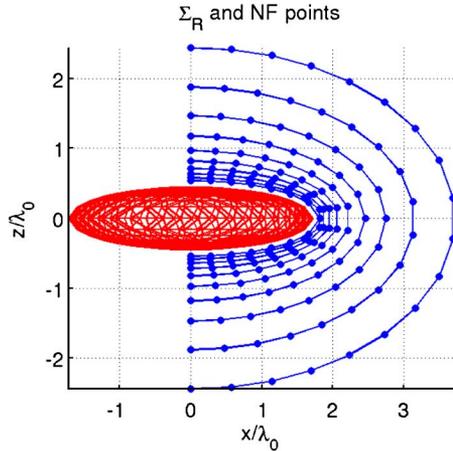
Fig. 2.   Depiction of $\Sigma_R$ and the curves for near-field comparison.
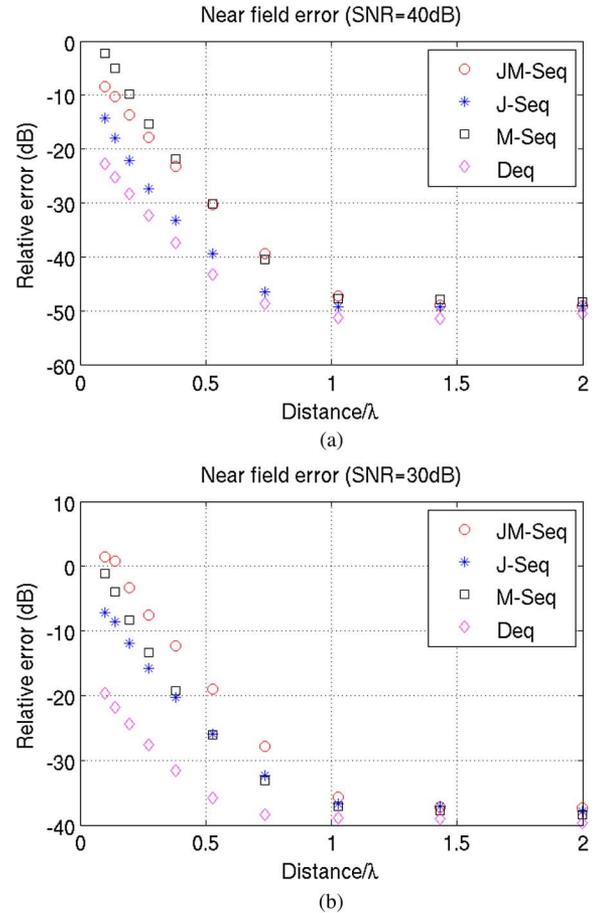


Fig. 3.   Near-field error as given by (4) for reconstruction from synthetic data with varying SNR levels. (a) Solver residuals: JM-SEqF $2.6 \cdot 10^{-6}$, J-SEqF $1.2 \cdot 10^{-5}$, M-SEqF $9.3 \cdot 10^{-6}$, and DEqF $1.2 \cdot 10^{-4}$. (b) Solver residuals: JM-SEqF $8.1 \cdot 10^{-6}$, J-SEqF $3.3 \cdot 10^{-5}$, M-SEqF $2.0 \cdot 10^{-5}$, and DEqF $2.1 \cdot 10^{-4}$.

sampling points depicted in Fig. 2. Synthetic data has the additional advantage of allowing the assessment of stability under various (known) conditions of signal-to-noise ratio (SNR); the latter represents actual (thermal) noise as well as unavoidable imperfections in measurements, like positioning/misalignment errors and probe effects beyond probe compensation. In Fig. 3, the near-field residuals are plotted for the various formulations and SNR levels considered of 40 and 30 dB.

Fig. 3 provides an interesting picture of the performance of the various formulations. A feature common to all formulations is the ability to reconstruct fields with a residual below the SNR at distances $\geq 1\lambda$ from $\Sigma_R$. This is a consequence of the limited spatial extent of the source, which is intrinsically enforced by any source reconstruction formulation and aids in removing "noise" due to sources outside $\Sigma_R$. An additional point of interest is the poorer performance of the M-SEqF with respect to the other formulations for $\mathrm{SNR} \geq 40$ dB (only the 40-dB case shown for brevity). Since only the electric field is measured, reconstruction in terms of M-SEqF only involves the MFIE operator; it can be conjectured that this is the cause of the lesser accuracy. On the other hand, the EFIE appears in all of the remaining formulations (in some, along with MFIE).

All results in Fig. 3 indicate a superior performance of DEqF over all the SEqFs for near-field prediction with realistic SNR levels. This superiority is more pronounced for: 1) smaller observation distances from $\Sigma_R$; and 2) increasing noise levels. It is seen that the difference is noticeable already at SNR of 40 dB, where DEqF achieves over 8 dB accuracy gain with respect to any of the SEqFs.

The results above mean that one must choose with care the formulation employed in applications requiring the accurate evaluation of the near fields, especially at distances $< 1\lambda$. This is the case, e.g., of antenna diagnostics, of electromagnetic compatibility (EMC)—especially in assessment of EM interference (EMI). For the diagnostics of antenna arrays, visualization of the contribution of each element is very important, and the need to displace $1\lambda$ outwards $\Sigma_R$ for an acceptable field accuracy means that only a smoothed version of the field sought after is available with SEqFs, which will entail the loss of crucial information [10], and especially so for sources of cross polarization.

The performance seen can be better understood by referring to the singular-value spectrum of the linear system arising for each of the formulations. These are shown in Fig. 4, where it is observed that the DEqF considerably improves conditioning even with respect to single-current formulations that have a halved number of unknowns. These results are in full agreement with the discussion on the spectrum of the operators involved in each of the formulations presented in [8]. As discussed there, the loss of accuracy is due to the poorer spectral properties of SEqFs; the noise captured in the solution of the ill-conditioned problem is filtered away only when the radiated field is computed at some distance, as observed. Note that the benefits of the DEqF are not limited to measurements in the far field, as in the present case. It was shown in [8] that the DEqF provides a considerable improvement of the spectrum also in the near-field case, albeit less pronounced as a result of the improved properties of the (near) radiation operator.

A more stable solution closer to the desired reconstruction surface with SEqFs could be obtained via some form of regularization. A large body of literature on this topic exists, but the main issues are the following. First of all, for a good tradeoff between information recovery and noise amplification, one needs—as a minimum—to know the SNR, which is not
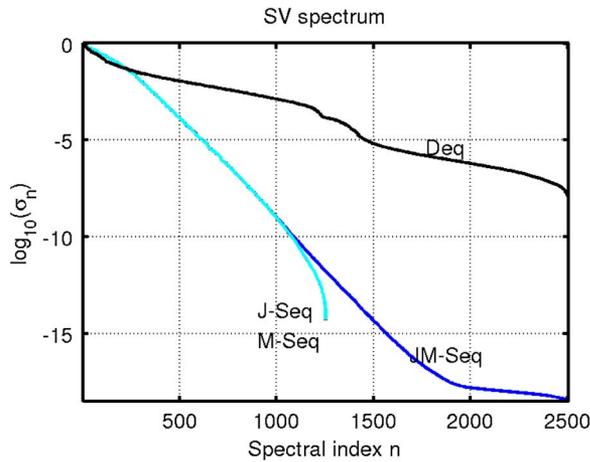
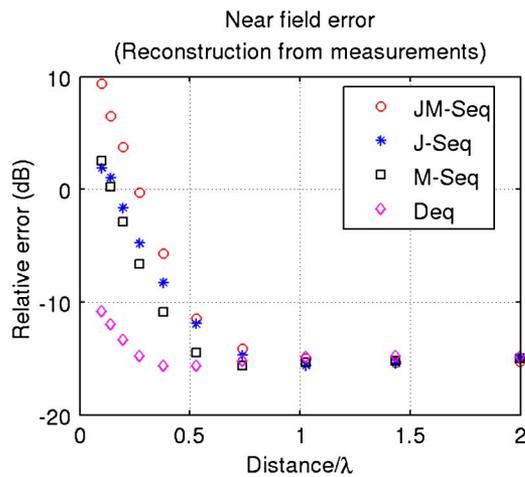Fig. 4. Spectrum of singular values for the reference problem considering all the formulations tested.



Fig. 5. Near-field error for reconstruction from measured data (reference: full-wave simulation). Solver residuals: JM-SEqF $1.2 \cdot 10^{-5}$, J-SEqF $3.8 \cdot 10^{-5}$, M-SEqF $3.8 \cdot 10^{-5}$, and DEqF $7.9 \cdot 10^{-4}$.

always available. More importantly, all regularizations always imply a smoothing (low-pass filtering) that does what radiation at some standoff distance also does, i.e., ultimately limiting the spatial resolution of source reconstruction near the desired reconstruction surface.

### B. Tests With Measured Data

We now turn attention to tests with measurements of a prototype of the structure considered. The reader is referred to [8] for details on the measurements and a comparison between synthetic and measured data at $\Sigma_M$. In absence of measured near-field reference data, we employ results from full-wave simulation as in the previous subsection to assess the accuracy of reconstruction. This is expected to introduce additional error because our CAD model lacked some of the feed details and neglected the spurious interaction with the supporting mast (this is likely to have a significant contribution in the lower hemisphere, where the screening effect of the ground plane leads to a low-level field).

Comparison between reconstructed near fields and the (full-wave) reference is shown in Fig. 5. It is seen therein that while performance is degraded for all formulations as expected from the approximations underlying reference data, DEqF provides a considerably better approximation to synthetic data (better than 12 dB improvement). The effect of this behavior in diagnostic applications was already demonstrated in [6].

## IV. CONCLUSION AND PERSPECTIVES

Analysis of various formulations of the source reconstruction problem show practically equivalent accuracy for fields reconstructed at one wavelength or greater away from the desired reconstruction surface $\Sigma_R$ around the AUT, meaning that all of them can be employed in NF–FF transformation applications and, with limitations, in some NF–NF transformations. In view of this, single-current formulations (J-SEqF and M-SEqF) are to be preferred in view of the halved number of unknowns and the presence of only one operator (either EFIE or MFIE), which impacts on implementation simplicity, computation time, and finally solution stability at realistic SNR. Among the single-current formulations, the use of J-SEqF appears more accurate when electric field measurements are used in reconstruction.

The situation is drastically changed when fields in the close vicinity of the actual radiators are required (i.e., distances $\leq 1\lambda$) as in typical diagnostic and EMC applications. Under these conditions, only DEqF [6] provides robust field reconstruction for a wide range of SNR, counterbalancing the additional implementation and computational complexity.

### REFERENCES

[1] C. Cappellin, A. Frandsen, and O. Breinbjerg, "Application of the SWE-to-PWE antenna diagnostics technique to an offset reflector antenna," *IEEE Antennas Propag. Mag.*, vol. 50, no. 5, pp. 204–213, Oct. 2008.

[2] Y. Alvarez, F. Las-Heras, and M. Pino, "Reconstruction of equivalent currents distribution over arbitrary three-dimensional surfaces based on integral equation algorithms," *IEEE Trans. Antennas Propag.*, vol. 55, no. 12, pp. 3460–3468, Dec. 2007.

[3] J. J. Laurin, J. F. Zurcher, and F. Gardiol, "Near-field diagnostics of small printed antennas using the equivalent magnetic current approach," *IEEE Trans. Antennas Propag.*, vol. 49, no. 5, pp. 814–828, May 2001.

[4] T. F. Eibert and C. H. Schmidt, "Multilevel fast multipole accelerated inverse equivalent current method employing Rao–Wilton–Glisson discretization of electric and magnetic surface currents," *IEEE Trans. Antennas Propag.*, vol. 57, no. 4, pp. 1178–1185, Apr. 2009.

[5] K. Persson and M. Gustaffson, "Reconstruction of equivalent currents using a near-field data transformation—With radome applications," *Prog. Electromagn. Res.*, vol. 54, pp. 179–198, 2005.

[6] J. Araque and G. Vecchi, "Improved-accuracy source reconstruction on arbitrary 3-D surfaces," *IEEE Antennas Wireless Propag. Lett.*, vol. 8, pp. 1046–1049, 2009.

[7] K. Persson, M. Gustafsson, and G. Kristensson, "Reconstruction and visualization of equivalent currents on a radome using an integral representation formulation," *Prog. Electromagn. Res. B*, vol. 20, pp. 65–90, 2010.

[8] J. A. Quijano and G. Vecchi, "Field and source equivalence in source reconstruction on 3D surfaces," *Prog. Electromagn. Res.*, no. PIER 103, pp. 67–100, 2010.

[9] M. Hanke, "The minimal error conjugate gradient method is a regularization method," *Proc. Amer. Math. Soc.*, vol. 123, no. 11, Nov. 1995.

[10] O. M. Bucci, L. Crocco, and T. Isernia, "Improving the reconstruction capabilities in inverse scattering problems by exploitation of close-proximity setups," *J. Opt. Soc. Amer. A*, vol. 16, no. 7, pp. 1788–1798, 1999.